

CHAPTER-I

SEMICONDUCTOR SUPERLATTICES AND THEIR PROPERTIES : AN INTRODUCTION

In this chapter we present a brief introduction to superlattices of various types and the modulation doping. A review of the work done on collective excitations, Light scattering, Electron-electron scattering and Electron-impurity scattering is also reported in this chapter. The review work is based on the recent work carried out on semiconductor superlattices.

1.1 Introduction to Semiconductor Compositional Superlattices

The fabrication of artificial structure materials such as superlattices has been possible through the advancement in growth techniques, like molecular beam epitaxy (MBE). A semiconductor superlattice (SL) consists of alternating layers of one or more semiconductors. Research on synthesized semiconductor superlattices was initiated with a proposal in 1969-1970 by Esaki and Tsu: a one-dimensional periodic structure consisting of alternating ultrathin layers, with its period less than the electron mean free path. In Figure 1.1, such a superlattice structure is shown. The electron mean free path, an important parameter for the observation of quantum effects, depends heavily on crystal quality and also on temperature and the superlattice period, layer thickness (determining width of potential wells or barriers), are reduced to less than the electron mean free path, the entire electron system enters into a quantum regime with the assumption of the presence of ideal interfaces, as illustrated in Fig. 1.1.

The introduction of the superlattice potential clearly perturbs the band structure of the host materials. The degree of such perturbation depends on its amplitude and periodicity. Since the superlattice period (d) is usually much greater than the original lattice constant, the Brillouin zone is divided into a series of minizones, giving rise to narrow allowed subbands separated by forbidden regions in the conduction band of the host crystal, as shown at the top of Fig. 1.2. Thus, this results in a highly perturbed energy-wave-vector relationship for conduction electrons, as schematically illustrated at the bottom of Fig. 1.2. Figure 1.3 shows the density of states $\rho(E)$ for electrons in a superlattice in the energy range including the first three subbands: E_1 between a and b , E_2 between c and d , and E_3 between e and f (indicated by arrow in the figure), to be compared with the parabolic curve for the three-dimensional electron system and the staircase like density

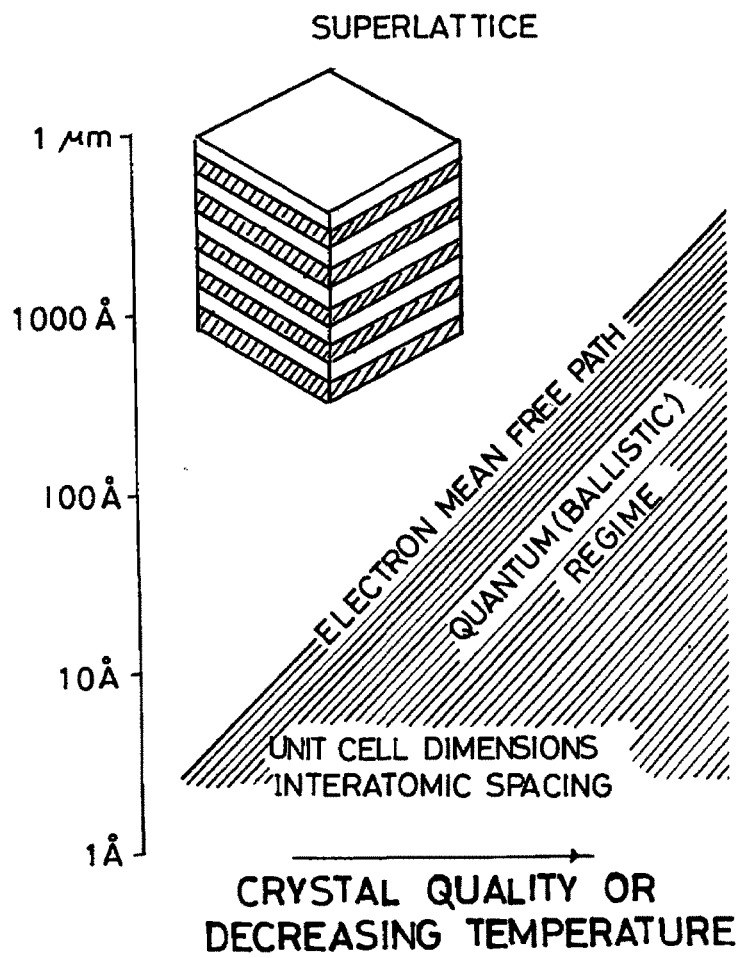


Fig.1.1 Schematic illustration of a quantum regime (hatched) with a Superlattice.

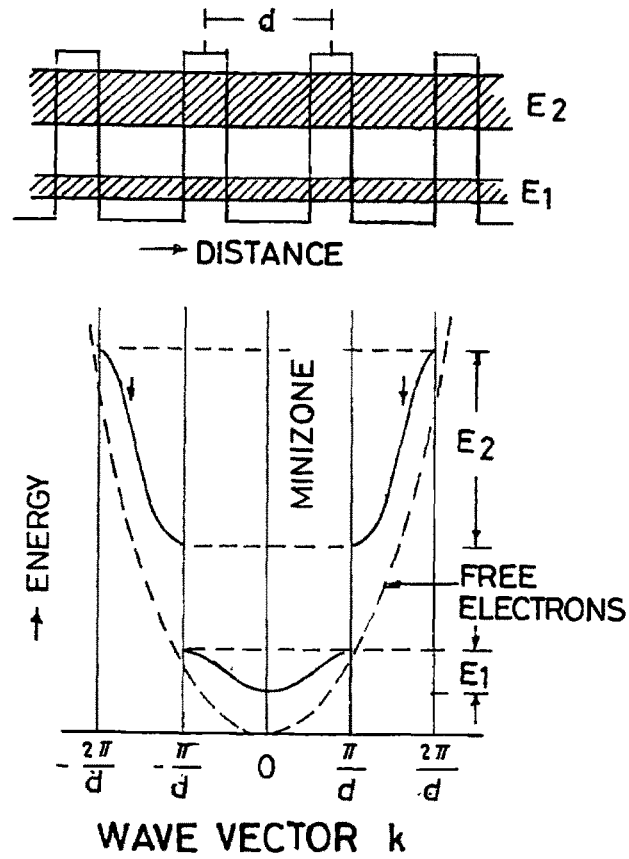


Fig.1.2 Potential profile of a superlattice (top) and its energy-wave relationship in the minizones.

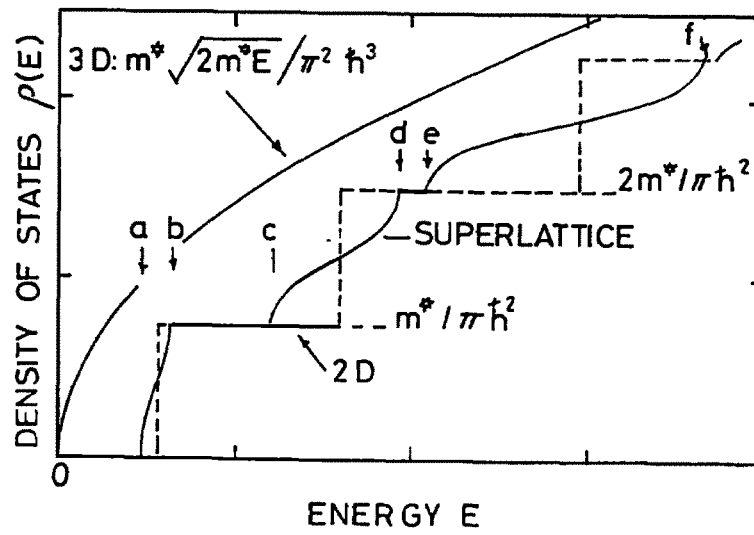


Fig.1.3 The comparison of the density of states for the three-dimensional and two-dimensional electron system with that of a superlattice.

of states for the two-dimensional system. Although the situation is analogous to the Kroning-Penney band model, it is seen here that the familiar properties are observed in a new domain of physical scale. In an extreme case, where quantum wells are sufficiently apart from each other, allowed bands become discrete states, and then electrons are completely two-dimensional, in which the density of states is illustrated by the dashed line in Fig. 1.3.

1.2 Types of Semiconductor Compositional Superlattices

The compositional superlattices consist of a periodic sequence of thin layers of alternating composition. The lattice parameters of two constituent layers in this superlattice are almost identical. There can be three types of compositional SL's depending upon matching of band gap at a heterointerface.

- (a) Type-I : GaAs/Al_xGa_{1-x}As Superlattice
- (b) Type-II : In_{1-x}GaAs/GaSb_{1-y}As Superlattice
- (c) Type-III : InAs/GaSb Superlattice.

(a) Type-I

In the type-I, the conduction and valence band-edge discontinuities ΔE_c and ΔE_v have opposite signs, and the energy gaps E_{g1} lies entirely within E_{g2} . In case of type-I superlattice it is found that the quantum well are formed for electrons within the smaller gap semiconductor layers. Hence, type-I SL's have a direct energy gap in real space.

(b) Type-II

In the type-II compositional SL's, the conduction and valence band-edge discontinuities ΔE_c and ΔE_v have the same sign and the energy gaps E_{g1} and E_{g2} overlap only partly or are separate. In this case, the quantum well for the electrons are formed by one material, while that for holes by other one. Hence type-II SL's have an indirect energy gap in real space.

(c) Type - III

The type-III or poly-type SL is a tripple constituent SL. Such a type of SL can be obtained by addition of AlsB layers in the InAs-Gasb system. In type-III SL (InAs/GaSb) separation of electrons and holes takes place due to the transfer of charge from wider gap, (GaSb) to smaller gap (InAs) because of unusual line up of energy bands. For layer thickness ($\leq 170 \text{ \AA}$), type III heterostructures are found to be semiconductor exhibiting spatial separation and confinement of electrons (in InAs) and holes in (GaSb) which are thermally excited. On the other hand for layer thickness ($>170 \text{ \AA}$) type III heterostructure behave as semimetal containing electrons (in InAs) and holes (in GaSb) even at zero temperature. Thus type III heterostructures offer a new class of materials where 2DEG formed in InAs coexists with a 2DHG of some density formed in GaSb side.

(d) Modulation Doping

In order to increase the number of free carriers in the superlattice, one dopes the GaAlAs system with a donor (usually Si) in GaAs/AlAs superlattice. This is reffered as modulation doping. The modulation doped SL's consist of periodic alternate electron layers. The main advantage of the modulation doping is the spatial separation of the quasi-free carriers from parent ionized impurities.

1.3 Doping Superlattices or n-i-p-i Structures

The doping SL's are composed of a periodic sequence of semiconductor layers of alternating doping. In the n-doped layers donor atoms contribute electrons, while the p-doped layers acceptor atoms bind electrons. Hence the periodic potential in doping SL's is exclusively space-charge induced. Doping SL's are homogeneous semiconductors which are modulated by the superpositon of the periodic superlattice potential. The doping superlattice differs from compositional supperlattice in a very important respect: their electronic properties are "tunable". This term means following: In doping superlattice band gap, subband structure, and carrier concentration are not only properties which can be predetermined by appropriate choice of the design parameters, but they become quantities which can be varied from outside within a wide range in

a given samples. Thus, doping superlattice form a new class of semiconductors in which the electronic properties are no longer fixed material parameters but tunable quantities. Apart from the possibility of designing a semiconductor with certain features, a property which compositional and doping superlattice have in common, the electric and optical properties for a given n-i-p-i crystals may be modulated within a wide range of values. Because of this tunability n-i-p-i crystals exhibits a lot of intriguing properties.

Moreover, such structure represents a particularly interesting model substance for the study of the properties of dynamically two-dimensional many-body systems with variable carrier concentration. The conductivity in doping superlattices differs in two fundamental points from their heterostructure counterparts:

1. The transport parallel to the layers is tunable within wide limits and generally involves electrons and holes.
2. The transport in the direction of periodicity in the case of n-i-p-i semimetals is dominated by electron-hole generation and recombination processes between n and players.

1.4 Strained Superlattices

The SL's considered hitherto are composed of lattice matched semiconductor materials. If the lattice-mismatch ($\Delta a/a$, being the lattices parameter) is larger than 0.5%, it is also possible to grow SL's with essentially no misfit dislocation by means of MBE. This is the case, in which the layer are thin enough that the lattice mismatch is accomodated entirely by homogenous strains of the layers. The homogenous strain induces some interesting modifications of the SL properties one example for strained-layer SL's is the GaSb-AlSb system with a lattice misfit of 0.7%. The strain induces a decrease of each band gap and a reversal of heavy - and light hole bands. This leads to a strong non parabolicity of the kane band structure. The well known example of strained superlattice is Si-Si_{1-x}Ge_x. Strain superlattice can differ from compositional superlattice in a very important manner. The lattice parameters of two constituent semiconductors in a compositional superlattice are almost identical, while the lattice parameters of consitituent semiconductor are not identical in strain superlattice.

1.5 Coupled Plasmon-Phonon Modes

The collective excitations in a quasi- two- dimensional electron gas and in type-I superlattices are used to predict the spectrum of inelastic light scattering by collective excitations. Light scattering experiments are at present the most important way to probe the collective excitations. Collective excitations in a two- dimensional electron gas (2DEG) have been studied extensively for the last couples of years. Following is the review of the work done on collective excitations in recent years.

Collective electron excitations of a two-dimensional square lattice has been studied by calculating a frequency and wave-vector-dependent dielectric function $\epsilon(q, \omega)$ within the random phase approximation by Latge et al. [1]. Both the dispersion relation of long-wavelength plasmons and the energy-loss function $\text{Im}[1/\epsilon(q, \omega)]$ has been numerically obtained for different values of the electronic concentration n_s . For low values of n_s results are described by the effective-mass approximation. As n_s increases, the Fermi level moves to regions in k-space where the band structure strongly deviates from that of free electrons, and the appearance of structure in the energy-loss spectrum can be observed. It is found that for all values of n_s , the long-wavelength behaviour of the plasma frequency, $\omega_p(q)$ can be described by a two-dimensional free-electron model provided a renormalized value of the electronic effective mass is introduced. Dimitril et al. [2] presented a theoretical study of the dielectric response and collective excitations of a two-dimensional system of bosons interacting via a dipolar interaction. They designed a model which simulates the situation occurring in semiconductor double quantum well systems under strong electric fields applied perpendicular to the layers. The applied field produces a net polarization of photoexcited electron and hole carriers and favours the appearance of long-lived polarized excitons. This gas of interacting point dipoles shows interesting features of low dimensional and statistics. Well defined density fluctuation excitations appear at low temperatures with a linear dispersion relation at long wavelengths. The low dimensionality of the system gives rise to an effective long ranged potential with only a faster power low decay.

The dielectric response of planar Fermi Plasma in the presence of a constant external magnetic field has been studied by Bardos and Frankel [3]. They derived conductivity tensor in the random phase approximation taking into account the effects of the spin of the electron.

Inclusion of spins makes a significant difference between this work and the previous studies, which ignored the intrinsic spin of the electron. In studying the dispersion relations for the electrodynamic modes of the plasma in an external magnetic field, it is necessary to observe that the longitudinal and transverse modes are coupled. These coupled modes have been investigated in some detail in this paper. The dielectric response of a planar Bose plasma in the presence of a constant external magnetic field has also been studied by calculations in the self-consistent random-phase approximation [4]. The tensor components dynamical conductivity are evaluated at zero temperature, leading to explicit dispersion relation for the electrodynamic modes of the plasma. For plasma layers, longitudinal and transverse modes are in general coupled, which has been investigated in detail.

Plasmon-phonon coupling in the doped short period $\text{GaAs}_n/\text{AlAs}_m$ tunneling superlattices was investigated [5]. Plasmon energy was shown to increase with barrier with decreasing, that rise phonon-plasmon coupling and charges localised phonon spectrum. Raman spectra observed may be interpreted as folding of plasmon-phonon dispersion calculated in Lindhard-Kermin approximation, weak electron tunneling causes shift of localized phonons energies. In case of two monolayer barrier, 3D-like behaviour of plasmons was observed. The density-density correlation function has been calculated for a modulation-doped GaAs/AlAs superlattice which was modelled to be an infinite periodic sequence of layers which consists of two dissimilar layers, one of GaAs and the other of AlAs, per unit cell [6]. The conduction electrons are assumed to be confined to GaAs layers. The calculation shows that, although the electron gas is confined in the GaAs layers, the plasma oscillations can interact with the lattice vibrations of both GaAs and AlAs. The interaction between AlAs lattice vibrations and the plasmons significantly contributes to the light-scattering spectrum. It was therefore argued that the experimentally measured frequencies of the coupled plasmon-phonon modes and their lineshapes for a modulation-doped GaAs/AlAs superlattice cannot correctly be described by the theoretical calculations which had been performed for a layered electron gas embedded in a homogenous dielectric background. The plasma oscillations of an electron gas and a hole gas in a GaAs doped superlattice were studied by Sharma & Sen [7]. The doped superlattice was modelled to be a one-dimensional periodic sequence of electron and hole layers embedded alternatively in a homogenous polar dielectric host medium. The density-density correlation function was calculated for a model structure in order to study the plasma-phonon coupled modes. The strong charge carrier - impurity scattering

which results from random doping impurities in the electron (hole) layers, was taken into account by choosing appropriate polarizabilities for intrasubband- intersubband transitions and the harmonic oscillator wave function as electron (hole) envelope functions. The calculation demonstrates that the presence of random doping impurities plasma modes in a GaAs doped superlattice can be observed for restricted values of wavevector. In the 2D limiting case, the plasma frequency in a doped superlattice is approximately proportional to $(q^2 - q_c^2)^{1/2}$ while for a modulation doped superlattice (such as $\text{Ga}_x\text{In}_{1-x}\text{As}/\text{GaAs}_y\text{Sb}_{1-y}$) it is proportional to q , for small q -values. q_c is the critical value of the in-plane wavevector q . They have also calculated lineshapes of coupled plasmon-phonon modes for doped superlattice.

A calculation of magnetoplasmons and their line shapes for a doped superlattice and a compositional type-II superlattice has been performed for the case when static magnetic field is applied along the direction of superlattice [8]. Calculation of polarizability of two-dimensional electron (hole) gas, for all possible transitions between Landau levels has been made. The frequencies of magnetoplasmons and their line shapes are then computed for a GaAs doped superlattice and for InAs/GaSb compositional superlattice for $0 \rightarrow 1$, $0 \rightarrow 2$ and $0 \rightarrow 3$ transitions by assuming that only ground Landau level ($n=0$) is filled. InAs/GaSb superlattice exhibits three bands of magnetoplasmons for each of electron as well as hole gas. In case of GaAs doped superlattice only one band of magnetoplasmons is obtained for holes, whereas three bands are obtained for electrons, because of high value of single particle scattering damping parameter for a doped superlattice as compared to that for a compositional superlattice. The computed line shapes of magnetoplasmons exhibit reasonable peak height and peak width which can be measured experimentally for right choice of values of superlattice parameters.

Some of the shortcomings of theoretical work done on plasmons and plasmon-phonon coupled modes in semiconductor superlattices are as follows; (i) single particle relaxation time was treated as a parameter in phenomenon-logical manner, (ii) dielectric and effective mass mismatch at heterointerface has been ignored and (iii) interaction of intrasubband and intersubband transition on varying period of a superlattice was not considered in a proper manner. This has been a motivation of our work on plasmons and plasmon-phonon coupled modes, which has been presented in this thesis.

1.6 Light Scattering in Superlattices

Several light scattering experiments has been performed on superlattices. Inelastic light scattering by electron excitations with large wave vectors in a 2D magnetoplasma has been studied by considering microscopic mechanism of inelastic light scattering in an interacting electron plasma in semiconductor heterostructure. In the dipole limit, the cross section consists of two main contributions : the first is related to a disorder induced mechanism and the second arises from the Coulomb interaction. The spectra of disorder-induced light scattering are described in terms of correlation function of a random potential. The spectrum induced by the Coulomb interaction arises from two-quasi particle excitations [9]. The calculation of low-frequency Raman scattering by longitudinal acoustic phonons in superlattices has been performed, where phonons are treated as elastic waves propagating in a continuum and their mode patterns has been calculated by a transfer-matrix method. The electromagnetic propagation was calculated neglecting reflections and refractions at the interfaces, through the use of the same index of refraction for both constituent materials. The use of a complex refraction index allows for absorption effects to be included [10]. A theoretical calculation of the Raman scattering cross section for palsmon-polaritons in a quasiperiodic superlattice that follows the Faboncci sequence has been carried out. The green functions,necessary to find the Raman cross section, has been determined by linear response theory. Numerical prediction of the Raman spectra are compared with recent experimental data [11]. Raman spectroscopy has been used to study intersubband transition in InAs/AlSb single quantum wells grown by molecular-beam epitaxy on (100) GaAs substrates using strain-relaxed AlSb or GaSb buffer layers [12]. From the measured energies of the coupled longitudinal optical phonon -intersubband plasmon modes the single particle transition energies between the first and second confined electron subbands were deduced as a function of the width of the pseudomorphically strained InAs well. Subband spacings calculated including the effects of strain and non-parabolicity were found to be in agreement with the experimental transition energies. For a given well width, the two-dimensional electron concentration deduced from Raman measurements was found to be lower than the concentration measured in the dark by Hall effect, but showed a significant increase with increasing optical excitation intensity. Raman scattering by longitudinal-optical (LO) phonon-plasmon coupled (LOPC) mode in carbon -doped p-type InGaAs with indium composition ($x=0.3$) and hole concentration from 10^{17} to 10^{19} - cm^{-3} grown by metal organic molecular beam epitaxy was studied experimentally [13]. Only one

LOPC mode appears between the GaAs-like and InAs-like LO modes was observed. The peak position of the LOPC mode is near the GaAs-like transverse-optical mode frequency and is insensitive to the hole concentration. The line width and intensity of the LOPC mode are dependent strongly on the carrier concentration, while the two LO modes decrease and become invisible under the high doping level. It was shown that plasmon damping effect plays a dominant role in Raman scattering by LOPC mode for the p-type InGaAs. Resonant Raman scattering by optic and acoustic phonons in GaAs/Al_xGa_{1-x}As multiple quantum wells in high magnetic fields has been studied by Ruf and Cross [14]. The Raman efficiency exhibit pronounced magneto-oscillations at interband transitions between Landau levels from which they determined nonparabolicity and anisotropy effects of the electron effective mass. Intersubband transitions in InAs/AlSb quantum wells has been studied by resonant Raman scattering [15]. For optical excitation in resonance with the E₁ band gap of InAs, both high-and low-frequency coupled longitudinal-optical phonon intersubband plasmon modes are observed. From the measured energies of these plasmon modes the single-particle transition energies between the first and second confined electron subband were deduced as a function of the InAs well width. Good agreement was found with subband spacings predicted by theory including the effects of strain and nonparabolicity. InAs/AlSb surface quantum wells, where a pseudomorphically strained InAs quantum well is grown on an AlSb buffer layer without an AlSb top barrier, also show well-resolved intersubband plasmon modes, indicating higher-electron mobilities than those typically found in the surface inversion region of thick InAs layers. Resonant Raman scattering was used to study an InSb/In_{1-x}Al_xSb strained-layer superlattice and the InSb and In_{1-x}Al_xSb parent materials [16]. Resonant enhancement peaks were observed in epilayer films in the regions of the E₁ and E₁+Δ₁ optical gaps. In the superlattice, two sets of peaks observed in the plots of the Raman cross section versus exciting photon energy are shown to originate from the independent electronic transitions in the alternating layers. The calculated resonance Raman profiles for two phonons in the alloy layers are in reasonable agreement with experiment. Raman scattering has been used to study a variety of InSb/In_{1-x}Al_xSb strained -layer superlattices grown by magnetron sputter epitaxy [17]. The observed frequencies of zone-folded longitudinal acoustic phonons agree well with those calculated using Rytov's theory of acoustic vibrations in layered media. The intensities of these phonons do not coincide with those calculated within the regime of the photoelastic mechanism for lighting scattering because the exciting light energy is close to resonance with superlattice electronic transitions. The longitudinal optic phonons in In_{1-x}Al_xSb layers exhibit two-mode behaviour and their shift due to intralayer strain is discussed

1.7 Electron-electron and Electron-impurity scattering and its implications

The effect of electron-electron (e-e) interaction on transport in bulk like systems of various dimensionalities is still an area of active research to this day, both experimentally [18,19] and theoretically [20,21]. On the face of it, it would seem that in the case of doped parabolic band semiconductor, where Unklapp processes are negligible, e-e scattering should not effect the linear transport properties of bulk like systems [purely quantum effects such a weak-localization corrections excepted], since an e-e scattering event conserves the total current in the system. Nevertheless, it has been appreciated for a long time that e-e scattering can affect the mobility of a system semiclassically by scattering carriers into or out of parts of the Brillouin zone that are strongly affected by the other available scattering mechanism [22,23]. Much work has been done in this field. Over the past several decades, two-dimensional electron systems (2DES) have been extensively studied for both their fundamental and technological interest. The 2DES in high mobility GaAs/Al_xGa_{1-x}As heterostructures has become an especially suitable systems for studying electron-electron scattering effects, because of the reduced effect of impurity scattering arising from the modulation-doping technique. Many properties of the 2DES are strongly influenced by the presence of electron-electron interactions. One most one most important property is the broadening of the electronic states by inelastic Coulomb scattering, which plays a major role in many physical process, such as tunnelling [24], ballistic hot electron, transport [25,26] and localization [27]. The asymptotic properties of Coulomb scattering in a 2DES are well established from the existing theoretical work [28-33]. The electron inelastic lifetime, τ in a pure 2DES becomes $\tau^{-1}(\xi) \propto \xi^2 \ln \xi$ for $\xi_F \gg \xi \gg k_B T$, and $\tau^{-1}(T) \propto T^2 \ln T$ for $\xi_F \gg k_B T \gg \xi$, where ξ is quasiparticle energy with respect to the Fermi energy ξ_F , k_B and T are the Boltzmann constant and temperature, respectively. Earlier experimental work on the inelastic lifetime of 2DES focused on the dephasing time [34], while the recent experiment on tunneling in a double quantum well structure directly measures the inelastic broadening [35]. The inelastic quasiparticle lifetime due to electron-electron interaction in a single loop dynamically screened Coulomb interaction within random-phase approximation has been calculated. It has been found that the excellent quantitative agreement with the inelastic scattering rates in the tunnelling experiment without any adjustable parameter [35]. Inelastic lifetime of confirmed two-component electron systems in semiconductor quantum-wire and quantum-well structures has been investigated theoretically [36]. It has been found that the scattering rate of a two-subband quantum wire is quite

different from that of a one-subband quantum wire because of momentum and energy conservations are less restrictive on scattering processes in two-subband systems where additional scattering channels are available. The inelastic Coulomb life time τ_{ee} of a quasiparticle near of the Fermi surface of a 2DES has been investigated [37]. It has been found that at low temperature $1/\tau_{ee}$ behaves like $T^2 \ln T$. At small quasi particle excitation energy, the leading contribution to $1/\tau_{ee}$ is inversely proportional to the electronic density and does not depend upon the electric charge. The role of electron-electron scattering in the dynamics of intersubband relaxation in GaAs quantum wells has been investigated theoretically [38]. The scattering rate has been calculated using the Fermi golden rule, as a function of the carrier densities. The dependence of the intersubband relaxation time on the quantum well width is also investigated. Results show that the electron-electron scattering increases linearly as a function of the carrier densities. Band-filling effect limits the efficiency of this mechanism under high carrier densities. Energy and temperature-dependent life time of an electron on a cylindrical Fermi surface has been investigated to study the influence of Fermi-surface geometry on the lifetime of an electron due to its interaction with other electrons. At zero temperature, the dominant energy dependence of the inverse lifetime or the decay rate is $\varepsilon^2 |\ln \varepsilon|$ for small values of the parameter ε , which is the electron energy relative to the Fermi energy. At finite temperature the decay rate leads to an electrical resistivity proportional to $T^2 |\ln kT/\mu|$ instead of the T^2 -dependence characteristic of a spherical Fermi surface, where μ is chemical potential. Similar calculations (using Fermi golden rule) for a spherical Fermi surface has also been done exactly at zero temperature [39]. Electron-electron relaxation time in heterostructure has been studied in two different double quantum-well systems by Reizer & Wilkins [40]. They considered both intralayer and interlayer screened electron-electron interaction and include a contribution beyond the simple golden-rule result. In particular they found that (i) including a non-golden-rule contribution of the same order in the interaction always reduces the rate, (ii) as a result the intralayer golden-rule contribution is significantly smaller than all published calculations, and (iii) while included interlayer scattering may increase the rate, it is still less than the measured rate in a wide double-quantum-well system. The inelastic electron-electron scattering rate in strongly coupled quantum wells has been investigated [41]. Both intrasubband and intersubband scattering processes has been considered. The theoretical results are compared with experimental data obtained from the analysis of the resistance resonance measured on GaAs/Al_xGa_{1-x}As heterostructures in the presence of an in-plane magnetic field. Electron-electron scattering in linear transport in two-dimensional systems has

been studied by Hu and Flensberg [42]. They described a method of electron-electron scattering, including full finite-temperature dynamical screening, exactly in the Boltzmann equation, for small deviations of the distribution function from equilibrium. Using this method, they calculated the distribution function and mobilities for electrons in GaAs quantum well. They found a well-defined crossover from μ_0 to μ_∞ (which can be significantly different from each other) when the e-e and impurity scattering mean free paths are equivalent. For certain parameter studied, e-e is responsible for reduction in the mobility of upto 40%. μ_0 to μ_∞ are mobilities without e-e interaction and with large e-e interaction, respectively

A study of relaxation time for electron-electron interaction in superlattice of type I and II has been performed by us, which is reported in chapter IV. Basic object of our study is to see the effect of intralayer and interlayer interactions in a superlattice.

References

- [1] A. Latge et al. Phys. Rev. **B 47**, 4798 (1992).
- [2] M. Dmitril et al. Phys. Rev. **B 50**, 8715, (1994).
- [3] D.C. Bardos and N.E. Frakel, Phys. Rev. **B 49**, 4096 (1993).
- [4] D.C. Bardos, D.F. Hines and N.E. Frankel, Phys. Rev. **B 49**, 4082 (1993).
- [5] M.D.Efremov et al. Semicond. Phys. **32**, 583, (1993).
- [6] A.C Sharma and A.K. Sood, J. Phys. Condens. Matt. **6**, 1553 (1994).
- [7] A.C. Sharma and R.Sen. J. Phys. Condens Matt. **7**, 9551 (1995).
- [8] A.C. Sharma, P. Tripathi, R.Sen & N. Jain J. Pure & Applied Phys. in press (1999).
- [9] A.O. Govorov, J. Exp. Theor. Phys. Vol. **85**, 565 (1995).
- [10] O. Pilla, K.M. Lemas, M. Montagna, Phys. Rev. **B 16**, 11845 (1994).
- [11] E.L. Albuquerque et al. Solid state commun. **99**, 311 (1996).
- [12] J. Wagner, J. Schmitz, D. Richards, J.D. Raston and P. Koidl, Solid state Electronic,**40**, 281 (1996).
- [13] Qi. Ming et al. J. Appl. Phys. **78**, 7265 (1995).
- [14] T. Ruf. A. Cros 11th Int. Cong., *High magnetic fields in the physics of semiconductors* cambridge, MA USA, **350**, (1994).
- [15] J. Wagner, J. Schmitz, F. Fuchs, J. D. Ralston and P. Koidl, Phys., Rev. **B51**, 8786 (1995).
- [16] V.P. Gnezdilov, D.J. Lockwood and J.B. Weble, Phys. Rev. **B 48**, 11234 (1993).
- [17] V.P. Gnezdilov, D.J. Lockwood and J.B. Weble, Phys. Rev. **B 48**, 11228 (1993).
- [18] L.W. Molenkamp and M.J.M. dejong, Phys. Rev. **B 49**, 5038 (1994).
- [19] V. Chabasseur-Molyneux et al., Phys. Rev. **B 51**, 1379, (1995).
- [20] B.A. Sanborn, Phys. Rev. **B 51**, 14256 (1995).
- [21] W.W. Schulz and P.B. Allen, Phys. Rev. **B 52** (1995).
- [22] C. Heming and E. Vogt, Phys. Rev. **B 101**, 944 (1956).
- [23] R.W. Keyes, J. Phys. Chem. Soids **6**, (1958).
- [24] S.Q. Murphy, J.P. Eisentein, L.N. Pfeiffer and K.W. West, Phys. Rev. **B 52**, 14825 (1995).
- [25] A. Palevski et al Phys. Rev. Lett **62**, 1776 (1989).
- [26] V. Chabasseur-Molyneux et.al., Phys. Rev. **B 51** 13793 (1995).

- [27] See, for example, P. Lee and T V. Ramkrishnan Rev Mod. Phys. **57**, 287 (1985), and the references there in.
- [28] G. F. Giuliani and J. J. Quinn, Phys. Rev **B 26**, 4421 (1982).
- [29] C. Hodges, H. Smith and J.W. Wilkins, Phys. Rev. **B 4**, 302 (1971)
- [30] H. Fuknyama and E. Aliranams, Phys. Rev. **B 27**, 5976 (1983).
- [31] A. V. Chaplik, Zh. Eksp. Teor. Fiz. **60**, 1845 (1971) [Sov. phys. JET P 33 997 (1971)].
- [32] G. Fasol, Appl. Phys Lett **59**, 2430 (1991).
- [33] Y. M. Malozovsky, S.M.Bose, and P. Longe, Phys. Rev. **B 47**, 15242 (1993).
- [34] A. Yacoby et al. Phys. Rev. Lett. **66**, 1938 (1991)
- [35] Lian Zheng and S. Das Sarma, Phys. Rev. **B 53**, 9964 (1996)
- [36] Lian Zheng and S. Das Sarma, phys. Rev. **B 54**, 13908 (1996).
- [37] Gabricle F. Giuliani and John J. Quinn, Phys. Rev. **B 26**, 4421 (1982).
- [38] Zhi Zhang etal Com. J. Phys. **74**, 5252 (1996)
- [39] Christopher Hodges, Henrik Smith, and J.W. Wilkins, Phys Rev. **4** 302 (1972).
- [40] Micheael Reizer and John W. Wilkins Phys. Rev. **B 55**, R7363 (1917).
- [41] M. Slutzky, O. Entin - Wohlman, Y. Berk, A. Palevski and H. Shtrikman, Phys. Rev. **B 53**, 4065 (1996)
- [42] Ben Yu-Kuang Hu and Karsten Flensberg, Phys. Rev. **B 53**, 10072 (1996).